Fission fragment angular distribution for the ^{19}F + ^{197}Au fusion-fission reaction at near-barrier energies

R. Tripathi,[1] K. Sudarshan,[1] S. Sodaye,[1] A. V. R. Reddy,[1] K. Mahata,[2] and A. Goswami[1,*]

[1]*Radiochemistry Division, Bhabha Atomic Research Center, Mumbai-400085, India*
[2]*Nuclear Physics Division, Bhabha Atomic Research Centre, Mumbai-400085, India*

Angular distribution of fission fragments have been measured for ^{19}F + ^{197}Au reaction at bombarding energies from 91 to 110 MeV. Fission fragment angular distributions have been calculated by transition state model with the transmission coefficients obtained using the coupled-channels theory. The calculated angular anisotropies are in good agreement with the experimental anisotropies. The experimental fission cross sections have also been reproduced on the basis of the coupled-channels theory. The results of angular distribution measurement do not show any significant contribution from quasifission as was reported in the literature based on the measurement of evaporation residues and mass distribution.

I. INTRODUCTION

Angular distribution is one of the important observables of nuclear fission. According to the transition state theory [1] fission fragment angular distribution is governed by the saddle point states of the fissioning nucleus. The theory is based on the assumption that the fission fragments separate along the symmetry axis of the fissioning nucleus and the orientation of the symmetry axis does not change beyond the saddle point. The projection K of the total angular momentum J on the symmetry axis is determined by the orientation of the symmetry axis with respect to the beam direction. In the case of the spin zero target-projectile system, the total angular momentum vector J lies in the plane perpendicular to the beam direction. When the excitation energy of the fissioning nucleus at the saddle point is high enough, a spectrum of K states is populated, and the statistical saddle point model (SSPM) of Halpern and Strutinsky [2] is used to explain the fission fragment angular distribution.

In the 1980's, there was a renewed interest in the angular distribution studies in heavy ion induced fission of the heavier systems at higher excitation energies and angular momenta [3]. The main interest was to study the fission of the systems, which did not have well-defined fission barrier (as in the case of fast fission) or systems having nuclear temperature comparable to the fission barrier [4]. The results of such studies were summarized in Ref. [5]. Based on these investigations it was concluded that, for the fissioning systems with $A \geqslant 230$ and $Z \geqslant 90$, if the entrance channel asymmetry is higher than the α_{BG} (Bussenaro-Gallone critical mass asymmetry) [6], the angular distribution of the fission fragments is consistent with the prediction of the SSPM. On the other hand, if the entrance channel asymmetry is less than α_{BG}, fusion is inhibited particularly at higher l values and angular anisotropy of the fission fragments in these cases is higher than that predicted by

the SSPM [7]. However such arguments do not hold true when spherical targets like Pb and Bi are used [8–10]. This shows the role of target deformation in the complete fusion of heavy nuclei. Angular distribution was thus considered to be the most important observable of fission, which could explicitly exhibit the effect of the entrance channel dynamics on fusion-fission.

In the 1990's, a series of investigations on fission fragment angular distribution were directed towards understanding the fusion process around the entrance channel Coulomb barrier [9,11,12]. It was observed that there is an increase in the angular anisotropy with decreasing beam energy near the Coulomb barrier. Hinde *et al.* [11] proposed that the collision of the projectile with the tips of the deformed target nucleus leads to quasifission, while collision with the sides of the target leads to complete fusion-fission. In the quasifission, the memory of the narrow entrance channel K distribution [7] is retained and therefore the angular anisotropy is higher than that predicted by SSPM. According to Swiatecki [13] quasifission is expected to occur when the contact configuration of the target and projectile is more elongated than the compound nucleus saddle point configuration. In such a situation, an extra-push energy is needed to reach the saddle point. In general heavy fissioning systems or systems with higher angular momentum are expected to have compact saddle point, and therefore are expected to undergo quasifission.

Berriman *et al.* [14,15] measured the evaporation residue cross sections and fission fragment mass distributions in ^{12}C + ^{208}Pb, ^{19}F + ^{197}Au, and ^{30}Si + ^{186}W leading to the formation of the same compound nucleus ^{216}Ra. It was observed that there is a suppression of evaporation residue formation in the case of ^{19}F + ^{197}Au and ^{30}Si + ^{186}W compared to the prediction of the statistical model. Further, higher width of the mass distribution for these two systems compared to that in the case of ^{12}C + ^{208}Pb was observed over the entire excitation energy range studied. The suppression in the residue formation and enhancement in the width of the mass distribution have been interpreted as the signature of quasifission in ^{19}F + ^{197}Au and ^{30}Si + ^{186}W systems. The occurrence of quasifission has been attributed to the lower

entrance channel mass asymmetry for the ^{19}F + ^{197}Au and ^{30}Si + ^{186}W systems compared to the α_{BG}. Enhanced width in the mass distribution below the barrier as a result of quasifission has also been reported by Ghosh *et al.* [16]. The measurement of fission fragment angular distribution at near-barrier energies in these systems could further substantiate the occurrence of quasifission. Hinde *et al.* have observed higher angular anisotropy compared to SSPM calculation in ^{16}O + ^{238}U system [11]. This observation was explained on the basis of quasifission resulting from the collision of the projectile with the tip of the deformed target nucleus. However, Nishio *et al.* have reported complete fusion in the collision of ^{16}O with tips of deformed ^{238}U nucleus at sub-barrier energies, based on the measurement of evaporation residue cross sections [17]. Ikezoe *et al.* [18] have studied fission fragment angular distribution in ^{19}F + ^{197}Au system at $E_{lab} = 100$, 135, and 160 MeV. However, this work does not provide much information about the angular distribution at near-barrier energies. In the present paper, results of the measurement of fission fragment angular distribution in ^{19}F + ^{197}Au reaction are reported. The measurements have been carried out in the beam energy (E_{lab}) range of 91 to 110 MeV ($E_{c.m.}/V_B = 0.99$ to 1.20; V_B is entrance channel Coulomb barrier). The results have been analyzed in terms of standard statistical theory.

II. EXPERIMENTAL

The experiments have been carried out at BARC-TIFR Pelletron accelerator, Mumbai, using ^{19}F beam of energy 91, 96, 100, 105, and 110 MeV. A self-supporting target of Au having a thickness around 500 μg/cm^2 was used for the measurement of the angular distribution. The incident beam was collimated with a 3 mm diameter collimator. The target was mounted at the center of a 1 m diameter scattering chamber. Single fission fragments were detected in the angular range of 20° to 165° using two Si-detector telescopes. The thickness of the ΔE detectors was about 10 and 14 μm. The ΔE detectors were backed by 300 μm thick E detectors. The distance of the telescopes from the target was about 10 cm. The signals from the ΔE detectors were used to trigger the gate of the ADC. A Si-detector was kept at 40° with respect to the beam at a distance of about 25 cm form the target to monitor the Rutherford scattering. The data of the Rutherford scattering were used for the normalization to obtain the absolute fission cross sections.

III. RESULTS AND DISCUSSION

The experimentally observed fission fragment angular distributions were transformed from laboratory to center-of-mass frame of reference assuming fission following complete fusion at all the beam energies. In the transformation from labortaory to center-of-mass frame of reference, the kinematics relevant for symmetric fission was considered with kinetic energies calculated form the prescription of Rossner *et al.* [19]. The fission differential cross sections were obtained after
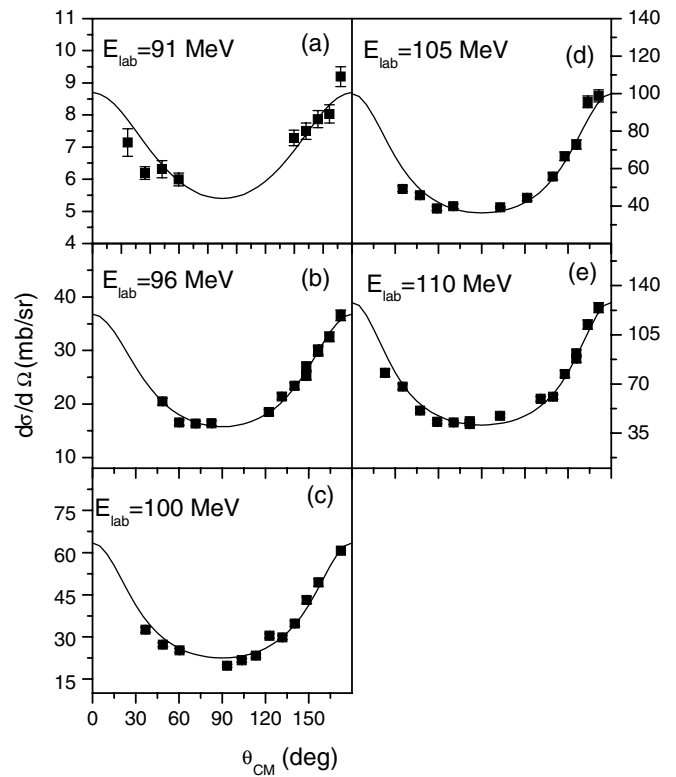

FIG. 1. Experimental fission fragment angular distribution in ^{19}F + ^{197}Au at (a) $E_{lab} = 91$ MeV, (b) $E_{lab} = 96$ MeV, (c) $E_{lab} = 100$ MeV, (d) $E_{lab} = 105$ MeV, and (e) $E_{lab} = 110$ MeV.

normalizing for the target thickness and beam current using the data of the monitor detector. Figures 1(a)–1(e) show the center-of-mass angular distributions of fission fragments in the ^{19}F + ^{197}Au reaction. The solid curves represent the best fits to the data obtained using the least square fitting procedure of Back *et al.* [3]. The procedure is based on the following expression of the angular distribution for a spin zero target-projectile system [3]:

$$W(\theta) = \sum_{J=0}^{\infty} (2J+1)T_J$$
$$\times \frac{\sum_{K=-J}^{J} \frac{1}{2}(2J+1)d_{0K}^{J}(\theta)^2 \exp\left[-K^2/2K_0^2\right]}{\sum_{K=-J}^{J} \exp\left[-K^2/2K_0^2\right]}, \quad (1)$$

where K_0^2 is the variance of K (projection of J on the nuclear symmetry axis) distribution. d_{0K}^{J} are the symmetric top wave functions which were calculated using the expressions given in Ref. [3]. T_J is the transmission coefficient for the fusion of the Jth partial wave. The fusion J distribution of the compound nucleus in the present work was calculated using the coupled channel code CCFUS [20]. The deformation data of the excited states of targets and projectiles for the coupled channel calculations were taken form Ref. [21]. The fusion J distribution was approximated as the J distribution of the fissioning nucleus for the calculation of angular anisotropy [$W(180)/W(90)$] using Eq. (1). K_0^2 was kept as a free parameter in the iterative fitting to the experimental data. The fitted curve was used to arrive at the experimental angular anisotropies.

In order to theoretically calculate the angular anisotropy, Eq. (1) was used with the K_0^2 calculated using the standard expression

$$K_0^2 = I_{\text{eff}} T / h^2, \qquad (2)$$

where I_{eff} is the effective moment of inertia of the fissioning nucleus at the saddle point given as

$$I_{\text{eff}}^{-1} = I_{\parallel}^{-1} - I_{\perp}^{-1}, \qquad (3)$$

where $I_{\parallel}$ and $I_{\perp}$ are moment of inertia for rotations about the symmetry axis and the axis perpendicular to the symmetry axis, respectively. The temperature T of the fissioning nucleus at the saddle point was calculated using Eq. (4):

$$T = \sqrt{(E^* - B_f - E_{\text{rot}} - E_\nu)/(A_f/8)}, \qquad (4)$$

where E^* is the excitation energy of the compound nucleus, B_f is the fission barrier, E_{rot} is the rotational energy, E_ν is the energy lost in the emission of presaddle neutrons, and A_f is the mass of the fissioning nucleus. I_{eff}, B_f, and E_{rot} were calculated using the rotating finite range model of Sierk [22]. The prescription of Kozuline *et al.* [23] was used to calculate the number of prefission neutrons (ν_{pre}). In the beam energy range studied, the ν_{pre} values varied from 1.45 to 2.20. Based on the studies of Rusanov *et al.* [24] it can be concluded that the compound nucleus in the present system will emit more than 80% of prefission neutrons before reaching the saddle point. Thus, in the present calculations the values of prefission neutrons were taken as presaddle neutrons. The ν_{pre} values were used to calculate E_ν at various bombarding energies. The calculated anisotropies are shown in Fig. 2 along with the experimental anisotropies. The angular distributions calculated using coupled and uncoupled J distributions (without considering the coupling of excited states of target and projectile) are shown as solid and dotted lines, respectively. It can be seen from the figure that the angular anisotropies calculated using the coupled channel J distributions are in good agreement with the experimental anisotropies, except at 100 MeV where the difference between the calculated and experimental value is slightly higher. The experimental angular distributions were integrated to obtain the fission cross sections. Figure 3 shows fission cross sections along with the fusion cross sections calculated using CCFUS. It is evident from the figure that the CCFUS calculations reproduce the experimental fission cross sections reasonably well. Thus both angular distributions and fission cross sections do not show any significant deviation from the fusion-fission process for the ^{19}F+^{197}Au over the excitation energy range of the present study, indicating absence of any significant contribution form quasifission.

From the extra-push model of Swiatecki [13] it is possible to explore the possibility of quasifission for a given target-projectile combination. In this approach there are three key configurations of the system, which play important role in the fusion process, namely, contact configuration, conditional saddle configuration, and usual saddle configuration. The contact configuration is defined as the one where the two nuclei are just in contact. As the contact configuration is reached the neck degree of freedom becomes unfrozen. The conditional
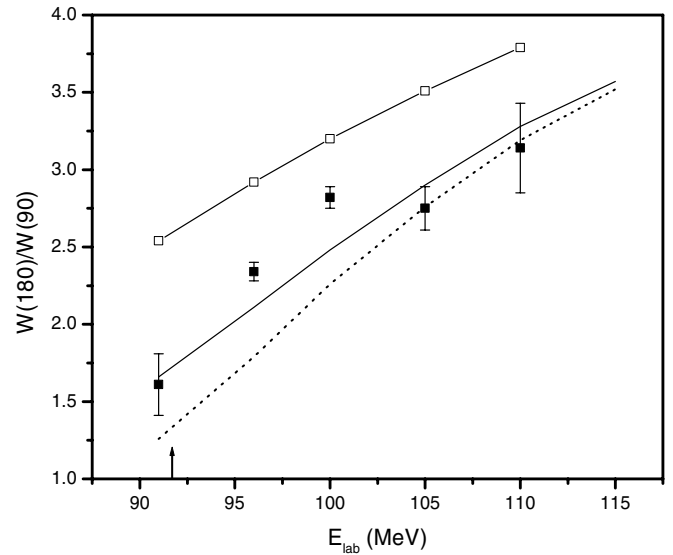

FIG. 2. Plot of experimental and calculated anisotropies in ^{19}F + ^{197}Au reaction. Solid squares are the experimental anisotropies and the hollow squares are the noncompound nucleus model [4] calculation using the fusion suppression data of Refs. [14] and [28]. Solid and dotted lines represent the angular anisotropies calculated using coupled and uncoupled J distributions, respectively. The arrow marks the entrance channel coulomb barrier.

saddle configuration corresponds to the maximum of the potential energy under the constraint that mass asymmetry remains frozen to its initial value. The third configuration is the usual compound nucleus saddle configuration, which is obtained when constraint on the mass asymmetry degree of freedom is removed. According to this model, if the contact configuration is less elongated than the conditional saddle configuration, the system will fuse to form the mononucleus. If the contact configuration is also less elongated than the usual
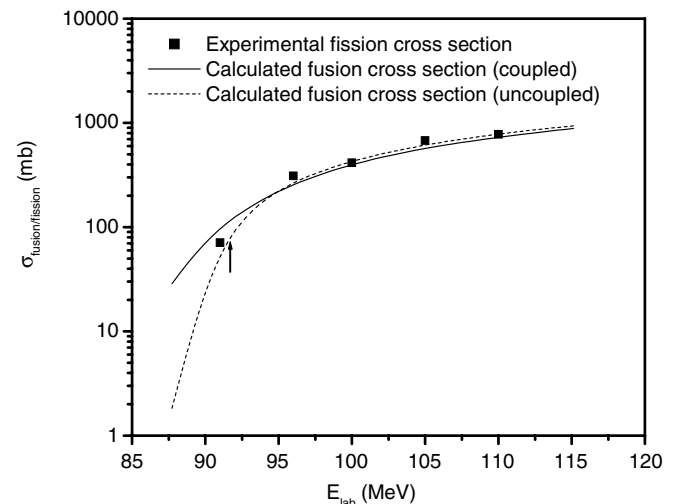

FIG. 3. Plot of experimental fission cross sections and fusion cross sections calculated using the code CCFUS [20] as a function of E_{lab}. The arrow marks the entrance channel coulomb barrier.
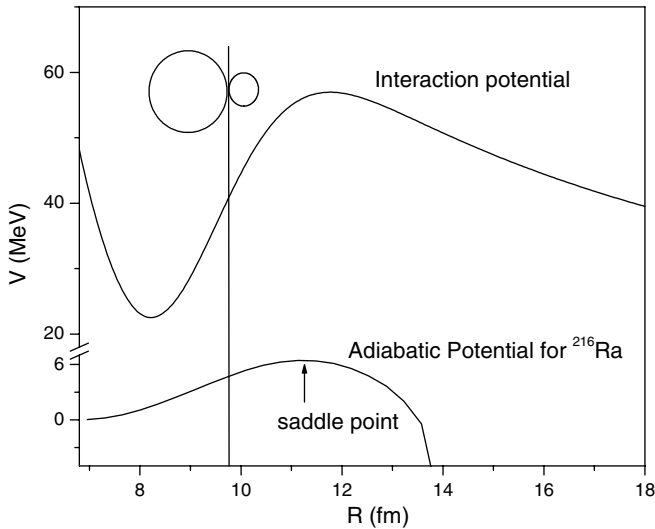
FIG. 4. Plot of interaction potential between ^{19}F and ^{197}Au and adiabatic potential for ^{216}Ra. The arrow marks the saddle point.

saddle configuration, the compound nucleus will necessarily be formed. However, if the contact configuration is more elongated than the saddle configuration, an extra-push energy will be required for the formation of the compound nucleus, otherwise the mononucleus will undergo quasifission. In order to explore the possibility of quasifission in the present systems, the adiabatic potential of the compound nucleus ^{216}Ra was calculated with respect to the elongation and the neck degrees of freedom using the procedure given in Ref. [25]. Figure 4 shows the plot of the adiabatic potential as a function of the elongation of the compound nucleus. The saddle point is marked by an arrow in the figure. The position of the contact configuration with respect to the usual saddle configuration is also shown in Fig. 4. It is evident form the figure that the contact configuration is well within the saddle configuration for the present system, and therefore will lead to the formation of the compound nucleus. According to Gregoire *et al.* [26] quasifission can be explained in terms of transition from the interaction potential in the entrance channel to the adiabatic potential in the exit channel. According to this model if the configuration corresponding to the minima in the entrance channel interaction potential (pocket configuration) is more compact compared to the saddle configuration, quasifission can be ruled out. The interaction potential between ^{19}F and ^{197}Au was calculated as a function of the inter-nuclear distance (R) using the formalism of Ref. [27] and is shown in Fig. 4. It can be seen from Fig. 4 that the pocket configuration is more compact compared to the saddle configuration, and therefore, the possibility of quasifission can be ignored.

Another model to explain the phenomenon of noncompound nucleus fission was proposed by Ramamurthy *et al.* [4]. According to this model if the entrance channel mass asymmetry is smaller than α_{BG}, the dinuclear system, after capture inside the conditional saddle point relaxes in mass asymmetry and elongation, passes over the unconditional fission saddle point, and moves towards the spherical compound nucleus [4,7]. Thermal diffusion during this phase can result in reseparation of the mass-equilibrated fragments over the

barrier leading to the occurrence of noncompound nucleus fission events. On the other hand, if the entrance channel mass asymmetry is higher than α_{BG}, the system, after capture inside the conditional saddle point, experiences a driving force towards larger asymmetries and smaller elongation, thus leading to the formation of the compound nucleus in a relatively shorter time scale. Even if the system reseparates before the formation of the compound nucleus, the asymmetry of the resultant products will be closer to or larger than the entrance channel asymmetry. Consequently, in these cases, noncompound nucleus fission events will not occur. Berriman *et al.* [14] have attributed the observed fusion suppression in the ^{19}F + ^{197}Au reaction to the lower entrance channel mass asymmetry compared to α_{BG} for the system. The model of Ramamuthy and Kapoor [4] gives a quantitative estimate of the effect of noncompound nucleus fission on fission fragment angular distribution. According to this model the fission fragment angular anisotropy is given by the following equation:

$$
\frac{W(0° \text{ or } 180°)}{W(90°)}
= \frac{(1 - P_{NCN})W_{CN}(0° \text{ or } 180°) + P_{NCN}W_{NCN}(0° \text{ or } 180°)}{(1 - P_{NCN})W_{CN}(90°) + P_{NCN}W_{NCN}(90°)},
$$

(5)

where P_{NCN} is the probability of noncompound nucleus fission events. $W_{CN}(\theta)$ and $W_{NCN}(\theta)$ represent the angular distribution of the fission fragments arising from the compound and noncompound nucleus processes, respectively. An approximate expression for the P_{NCN} is given in the following [4]:

$$
P_{NCN} = e^{-0.5B_f/T}.
$$

(6)

According to Eq. (6), contributions from the noncompound nucleus fission decrease exponentially with increasing ratio of the fission barrier to the temperature of the fissioning system. The expected contribution form the noncompound nucleus fission in the ^{19}F + ^{197}Au reaction varies from 5–12% over the excitation energy range of the present study. However, Berriman *et al.* [14] and Sagaidak *et al.* [28] have reported a constant value of P_{NCN} as ~0.36 in the ^{19}F + ^{197}Au reaction in the similar range. In order to study the effect of noncompound nucleus fission on the fission fragment angular distribution, a constant value of P_{NCN} as 0.35 from Ref. [28] was used for the calculation of the angular anisotropy using Eq. (5). $W_{NCN}(\theta)$ was calculated using Eq. (1) in which the variance of K distribution (K_0^2) for the compound process was replaced by the variance of K distribution (σ_K^2) for the noncompound nucleus fission. For the noncompound nucleus fission events the variance of K distribution is given by the following equation:

$$
\sigma_K^2 = J^2 \sigma_\theta^2,
$$

(7)

where σ_θ^2 is the angular variance representing the misalignment of the symmetry axis of the fused composite system with respect to $K = 0$ plane. Ramamurthy *et al.* [4] obtained a value of σ_θ^2 as 0.06 by fitting the fission fragment angular distribution in the systems having contribution from noncompound nucleus

fission. This value of σ_θ^2 has been used in Eq. (7) for the calculation of σ_K^2. The angular anisotropies calculated after considering the contribution from noncompound nucleus fission are shown in Fig. 2 as hollow squares. It is evident form the figure that the angular anisotropies expected from the P_{NCN} values from the evaporation residue measurement [14,28] are significantly higher than the experimental anisotropies. Thus the angular distribution results do not show any significant contribution from quasifission. The measurement of the correlation between the fission fragment mass and their emission angle in ^{19}F induced fission of ^{197}Au by Ikezoe *et al.* also showed that the contribution from quasifission is not significant at $E_{\text{lab}} = 100$ MeV [18]. The results on fission fragment angular distribution also indicate that the 100 MeV data agree with SSPM calculation. This is consistent with the observation in the present work.

IV. CONCLUSIONS

The present study shows that the statistical saddle point model can successfully explain the experimental fission fragment angular distributions for ^{19}F + ^{197}Au at near-barrier energies after considering the effects of coupling on the near-barrier fusion. These results indicate that the contribution from quasifission in the present system is not significant. This is in contradiction to the observation of quasifission by Berriman *et al.* [14] in the ^{19}F + ^{197}Au reaction at the beam energies comparable to that of the present system.

[1] R. Vandenbosch and J. R. Huizenga, *Nuclear Fission* (Academic, New York, 1973).

[2] I. Halpern and V. M. Strutinsky, in *Proceedings of the Second United Nations International Conference on Peaceful Uses of Atomic Energy, Geneva, 1958*, edited by J. H. Martens *et al.* (United Nations, Switzerland, 1958), Vol. 15, p. 408.

[3] B. B. Back, R. R. Betts, J. E. Gindler, B. D. Wilkins, S. Saini, M. B. Tsang, C. K. Gelbke, W. G. Lynch, M. A. McMahan, and P. A. Baisden, Phys. Rev. C **32**, 195 (1985).

[4] V. S. Ramamurthy and S. S. Kapoor, Phys. Rev. Lett. **54**, 178 (1985).

[5] Swaminathan Kailas, Phys. Rep. **284**, 381 (1997).

[6] U. L. Businaro and S. Gallone, Nuovo Cimento **5**, 315 (1957); K. T. R. Davies and A. J. Sierk, Phys. Rev. C **31**, 915 (1985).

[7] V. S. Ramamurthy *et al.*, Phys. Rev. Lett. **65**, 25 (1990).

[8] C. R. Morton, D. J. Hinde, J. R. Leigh, J. P. Lestone, M. Dasgupta, J. C. Mein, J. O. Newton, and H. Timmers, Phys. Rev. C **52**, 243 (1995).

[9] Huanqiao Zhang, Zuhua Liu, Jincheng Xu, Kan Xu, Jun Lu, and Ming Ruan, Nucl. Phys. **A512**, 531 (1990).

[10] A. M. Samant, S. Kailas, A. Chatterjee, A. Shrivastava, A. Navin, and P. Singh, Eur. Phys. J. A **7**, 59 (2000).

[11] D. J. Hinde, M. Dasgupta, J. R. Leigh, J. P. Lestone, J. C. Mein, C. R. Morton, J. O. Newton, and H. Timmers, Phys. Rev. Lett. **74**, 1295 (1995).

[12] R. Vendenbosch, Annu. Rev. Nucl. Part. Sci. **42**, 447 (1992).

[13] W. J. Swiatecki, Phys. Script **24**, 113 (1981).

[14] A. C. Berriman, D. J. Hinde, M. Dasgupta, C. R. Morton, R. D. Butt, and J. O. Newton, Nature (London) **413**, 144 (2001).

[15] D. J. Hinde, A. C. Berriman, R. D. Butt, M. Dasgupta, I. I. Gontchar, C. R. Morton, A. Mukherjee, and J. O. Newton, J. Nucl. Radiochem. Sci. **3**, 31 (2002).

[16] T. K. Ghosh, S. Pal, T. Sinha, S. Chattopadhyay, P. Bhattacharya, D. C. Biswas, and K. S. Golda, Phys. Rev. C **70**, 011604(R) (2004).

[17] K. Nishio, H. Ikezoe, Y. Nagame, M. Asai, K. Tsukada, S. Mitsuoka, K. Tsuruta, K. Satou, C. J. Lin, and T. Ohsawa, Phys. Rev. Lett. **93**, 162701 (2004).

[18] H. Ikezoe *et al.*, Z. Phys. A **330**, 289 (1988).

[19] H. H. Rossner, J. R. Huizenga, and W. U. Schröder, Phys. Rev. Lett. **53**, 38 (1984).

[20] C. H. Dasso and S. Landowne, Comput. Phys. Commun. **46**, 187 (1987).

[21] S. Raman, C. H. Malarkey, W. T. Milner, C. W. Nestor, Jr., and P. H. Stelson, At. Data Nucl. Data Tables **36**, 1 (1987).

[22] Arnold J. Sierk, Phys. Rev. C **33**, 2039 (1986).

[23] E. M. Kozuline, A. Ya. Rusanov, and G. N. Smirenkin, Phys. At. Nucl. **56**, 166 (1993).

[24] A. Ya. Rusanov, M. G. Itkis, and V. N. Okolovich, Phys. At. Nucl. **60**, 683 (1997).

[25] M. Brack, Jens Damgaard, A. S. Jensen, H. C. Pauli, V. M. Strutinsky, and C. Y. Wong, Rev. Mod. Phys. **44**, 320 (1972).

[26] C. Gregoire, C. Ngo, and B. Remaud, Phys. Lett. **B99**, 17 (1981); Nucl. Phys. **A383**, 392 (1982).

[27] H. Ngo and C. Ngo, Nucl. Phys. **A348**, 140 (1980).

[28] R. N. Sagaidak *et al.*, Phys. Rev. C **68**, 014603 (2003).